Potential Signature of a Kosterlitz-Thouless Transition in $BaNi_2V_2O_8$

M. Heinrich,[1] H.-A. Krug von Nidda,[1] A. Loidl,[1] N. Rogado,[2] and R. J. Cava[2]

[1]*Experimentalphysik V, Elektronische Korrelationen und Magnetismus, Institut für Physik, Universität Augsburg, D-86135 Augsburg, Germany*

[2]*Department of Chemistry and Princeton Materials Institute, Princeton University, Princeton, New Jersey 08544, USA*

(Received 25 February 2003; revised manuscript received 8 July 2003; published 26 September 2003)

ESR measurements are reported for the quasi-two-dimensional honeycomb antiferromagnet $BaNi_2V_2O_8$. Planar anisotropic properties are confirmed by angular dependent investigations of resonance field and linewidth. The divergence of the temperature-dependent linewidth on approaching T_N from above is described in terms of the Kosterlitz-Thouless transition, the critical behavior close to long-range magnetic order, and the 2D Heisenberg antiferromagnet. We provide arguments that the Kosterlitz-Thouless scenario is compatible with the observed critical exponent and suggest $BaNi_2V_2O_8$ is a weakly anisotropic 2D Heisenberg antiferromagnet.

DOI: 10.1103/PhysRevLett.91.137601 PACS numbers: 76.30.–v, 73.90.+f, 75.30.Kz

Investigations on a large number of layered compounds pointed out that the interpretation of experimental results concerning the critical behavior at the magnetic phase transition on two-dimensional (2D) materials is sophisticated [1,2]. In the case of an ideal 2D Heisenberg magnet a phase transition to long-range magnetic order does not exist at finite temperature [3]. For the two-dimensional XY model, Kosterlitz and Thouless (KT) and independently Berezinskii predicted a topological phase transition caused by the unbinding of vortex-antivortex pairs at the transition temperature $T_{KT} \neq 0$ [4–7]. However, real layered magnetic compounds are situated between these two ideal cases and exhibit a phase transition to three-dimensional (3D) long-range order at a finite temperature T_N often too large to be exclusively caused by the weak *interlayer* coupling, while anisotropies in the *intralayer* coupling seem to be more likely to explain the fundamental mechanism of ordering in layered antiferromagnets (AFM) [8,9]. In this respect the KT transition becomes a phenomenon which is not strictly confined to the XY model. Using the XXZ model Cuccoli *et al.* arrived at the conclusion that even an arbitrary small easy-plane anisotropy perturbing the isotropic 2D Heisenberg model can induce a KT transition at finite temperature [10,11]. By means of recent quantum Monte Carlo simulations [12,13] they predicted that quantum AFMs on a square lattice with very weak easy-plane exchange anisotropy display a crossover from a high-temperature isotropic behavior to a genuinely 2D XY behavior at a temperature t_{co} ($t = k_B T/J\tilde{S}^2$, $\tilde{S} = S + 1/2$) around 30% above the critical temperature t_{KT}. Slightly above t_{KT} 3D ordering is induced at t_N by the incipient intralayer KT transition [12]. In the specific heat this crossover appears in a small temperature region, well above the estimated transition temperature, as an anomaly in the form of a tiny peak. At the same time the susceptibility develops an anisotropy which increases to lower temperatures as already experimentally confirmed [12]. Even in an isotropic 2D Heisenberg AFM a KT transition can be induced at a finite temperature by an applied magnetic field, so that a genuine XY behavior can be observed in an extended temperature range [14]. Therefore, quasi-two-dimensional layered compounds with weak interplane interactions are good candidates to verify the behavior expected near a KT transition, e.g., $MnPS_3$ [15,16] and $BaNi_2P_2O_8$ [17–19]. Here we present electron-spin resonance (ESR) measurements on $BaNi_2V_2O_8$, which is isostructural to the latter compound and hence may exhibit a KT transition. In this compound ESR directly probes the spin dynamics of the Ni^{2+} spin and therefore is able to obtain important information on the critical behavior close to the magnetic phase transition.

$BaNi_2V_2O_8$ crystallizes with a rhombohedral unit cell (space group $R\bar{3}$, No. 148), which contains magnetic layers of edge-sharing NiO_6 octahedra (Ni^{2+}: spin $S = 1$) arranged on a honeycomb lattice (cf. Fig. 1) and separated by nonmagnetic layers of $V^{5+}O_4$ tetrahedra and Ba^{2+} ions. The growth of $BaNi_2V_2O_8$ single crystals is described in Ref. [20], where also the results of x-ray diffraction, susceptibility, specific-heat, and neutron-diffraction measurements are presented. The lattice parameters have been determined as $a = 5.028\ 99(4)$ Å and $c = 22.3450(2)$ Å (perpendicular to the magnetic layers) [20]. The difference of the intralayer Ni^{2+}-Ni^{2+} distance $d_1 = 2.9$ Å to the interlayer distance $d_2 = 2.57d_1$ is large; the AFM intralayer exchange interaction $J/k_B = -96$ K is much stronger than is seen in the isostructural compounds $BaNi_2P_2O_8$ and $BaNi_2As_2O_8$ [2]. The susceptibility exhibits a broad maximum near 125 K indicating low-dimensional ordering. For $T > 100$ K the compound behaves isotropically. At lower temperatures it becomes anisotropic for magnetic fields parallel and perpendicular to the NiO_6 layers. 3D AFM ordering occurs at $T_N = 50$ K determined by neutron scattering [20]. The Ni^{2+} spins are aligned antiferromagnetically within the planes with their three nearest Ni^{2+} neighbors, and they are also

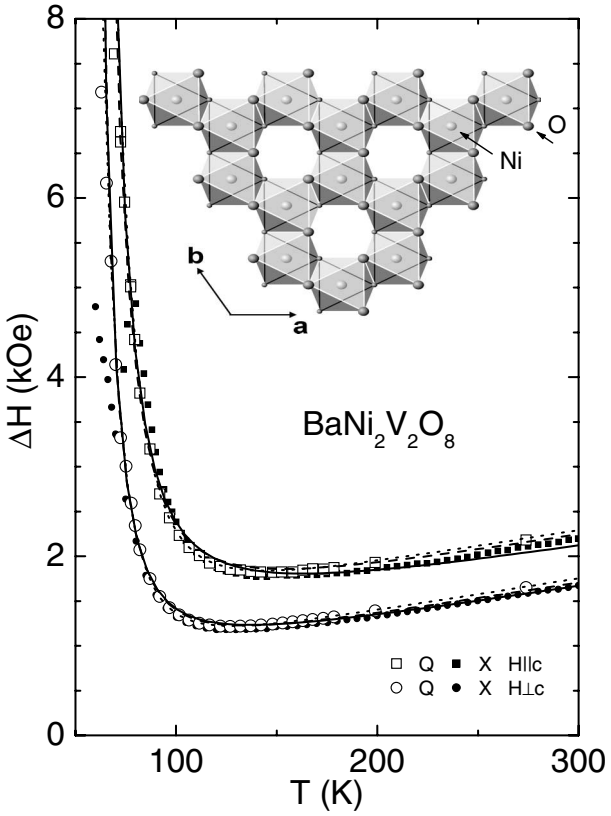

FIG. 1. Temperature dependence of the ESR linewidth ΔH of a $BaNi_2V_2O_8$ single crystal for the c axis parallel and perpendicular to the external magnetic field H at the Q-band (open symbols) and the X-band frequency (closed symbols). Solid lines: fits with Eq. (1), dashed lines: fits with Eq. (3), and dotted lines: fits with Eq. (4).

coupled antiferromagnetically between adjacent layers. However, the 3D ordering is only weakly observable in magnetic susceptibility and heat-capacity experiments. The specific heat exhibits a small feature at about 50 K and shows that most of the entropy was lost above T_N.

These properties show a striking similarity to the behavior theoretically predicted for weakly anisotropic AFMs [12,13] mentioned above. Although the calculations have been performed for systems on a square lattice with spin $S = 1/2$, the agreement is remarkable and a spin value $S = 1$ probably causes a shift of the transition temperatures t_{KT} and t_{co} to higher values as derived for the extreme cases of the isotropic Heisenberg and the XY model [21,22]. This argues for $BaNi_2V_2O_8$ being a weakly anisotropic 2D Heisenberg AFM.

The ESR measurements were performed on a Bruker ELEXSYS E500-CW spectrometer equipped with continuous-flow He cryostats (Oxford Instruments) at X-band (9.4 GHz) and Q-band (34 GHz) frequencies in the temperature range 4.2–300 K. The $BaNi_2V_2O_8$ single crystal was fixed in a quartz tube with paraffin in different orientations to the applied external magnetic field.

At high temperatures the ESR spectra in $BaNi_2V_2O_8$ consist of a broad resonance line of Lorentzian shape, which broadens very strongly with decreasing temperature and finally vanishes on approaching the magnetic ordering transition at $T_N \approx 50$ K. Resonance field H_{res} and linewidth ΔH (half width at half maximum) have been determined by numerical fitting of the spectra, as described, e.g., in Ref. [23]. Rotating the external magnetic field from the direction perpendicular to the magnetic planes ($H||c$ axis) to the orientation parallel to these planes the linewidth follows a $\cos^2(\theta)$ dependence (θ denotes the angle between the c axis and the magnetic field) with values between 2.1 and 1.2 kOe at 120 K. Simultaneously, the resonance field varies slightly. The g values are 2.225 ($H||c$) and 2.243 ($H \perp c$), respectively. There is no angular variation of linewidth and resonance field for the external field applied within the magnetic planes.

Figure 1 shows the temperature dependence of the ESR linewidth for $50 < T < 300$ K measured at X-band and Q-band frequencies. The results for both frequencies nearly coincide except for the temperature range in which the line becomes very broad. In that region, the values obtained at 34 GHz are more precise and can be analyzed up to a value of about 8 kOe due to the higher resonance field. For all orientations of the sample with respect to the external magnetic field the same kind of divergence is observed. For temperatures $120 < T < 300$ K, the linewidth increases linearly with increasing temperature, with a slope of $m = 3.62$ Oe/K and residual linewidths of $\Delta H_0 = 640$ Oe ($H \perp c$) and $\Delta H_0 = 1120$ Oe ($H||c$), respectively. Below 120 K, the linewidth exhibits a minimum of about 1800 Oe for $H \parallel c$ and 1200 Oe for $H \perp c$ and broadens very quickly on further decreasing the temperature until the signal becomes undetectable. The temperature dependence of the ESR linewidth observed in the 2D $S = 1/2$ AFM $Cu(HCOO)_2 \cdot 4H_2O$ [24,25] is very similar to the results for $BaNi_2V_2O_8$: For that compound the linear behavior at higher temperatures has been attributed to single-phonon absorption and emission processes. The same explanation probably holds for $BaNi_2V_2O_8$ with the higher residual linewidth due to the influence of the crystal field on $S = 1$ Ni^{2+}.

To characterize the divergent behavior on approaching T_N, we analyzed the temperature dependence of the linewidth in $BaNi_2V_2O_8$ in the context of (a) the KT transition, (b) classical critical behavior close to a magnetic phase transition, and (c) in terms of the 2D Heisenberg AFM.

In the case of the two-dimensional XY model, the temperature dependence of the ESR linewidth, disregarding the temperature dependence of the vortex velocity, is proportional to the cube of the correlation length ξ. The contribution of the out-of-plane correlations is negligible [5,17]. Adding a linear term to describe the high-temperature behavior, the linewidth should

follow the equation

$$\Delta H = A \exp\left(3b \Big/ \sqrt{\frac{T}{T_{\mathrm{KT}}} - 1}\right) + \underbrace{mT + \Delta H_0}_{\Delta H_{\mathrm{lin}}}, \quad (1)$$

with the Kosterlitz-Thouless temperature T_{KT} and $b = \pi/2$. Theoretical predictions for more realistic spin systems [26] allow the parameter b in Eq. (1) to be much smaller. This was confirmed by NMR [18] and ESR [17] measurements on the isostructural compound $BaNi_2P_2O_8$, which yielded a value of $b \approx 0.9$.

Applying Eq. (1), with m fixed to the high-temperature value, and $b = \pi/2$, fits the temperature-dependent linewidth of $BaNi_2V_2O_8$ for $H \perp c$ with $T_{\mathrm{KT}} = 43.3$ K, $A = 8.7$ Oe, and $\Delta H_0 = 525$ Oe. The result is shown as a solid line in Fig. 1. The same values for m, b, and T_{KT} result in a satisfactory description of the temperature dependence of the linewidth for $H \parallel c$ as well, yielding $A = 17.8$ Oe and $\Delta H_0 = 913$ Oe. The linear plot of $\ln(\Delta H_{\mathrm{div}}) = \ln(\Delta H_{\mathrm{ESR}} - \Delta H_{\mathrm{lin}})$ vs $-(T/T_{\mathrm{KT}} - 1)^{-0.5}$ shown in the upper frame of Fig. 2 demonstrates the good agreement of fit and data in the temperature range $65 < T < 160$ K. At lower temperatures the experimental values may be not precise enough due to the large linewidth, and at higher temperatures the misfit can be caused by a decreasing number of vortices.

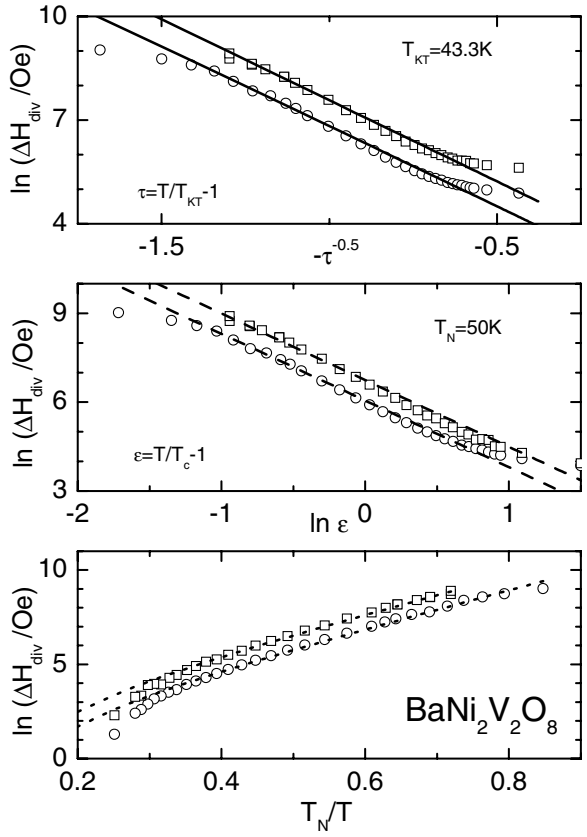

FIG. 2. Upper frame: plot of $\ln(\Delta H_{\mathrm{div}}) = \ln(\Delta H_{\mathrm{ESR}} - \Delta H_{\mathrm{lin}})$ vs $-(T/T_{\mathrm{KT}} - 1)^{-0.5}$, middle frame: plot of $\ln(\Delta H_{\mathrm{div}})$ vs $\ln(T/T_{\mathrm{N}} - 1)$, and lower frame: plot of $\ln(\Delta H_{\mathrm{div}})$ vs T_{N}/T (data and fits).

From the first results the interplane interaction J' in $BaNi_2V_2O_8$ can be estimated: According to Bramwell and Holdsworth [16,27], who have developed a theory for a system with weak in-plane anisotropy and interplane coupling, the following relation holds:

$$\frac{T_{\mathrm{N}} - T_{\mathrm{KT}}}{T_{\mathrm{KT}}} = \frac{4b^2}{[\ln(J/J')]^2}. \quad (2)$$

This is valid even for weakly anisotropic quantum models [13]. Using our experimental values, Eq. (2) yields $J/J' \approx 3000$, a result comparable to that observed for the isostructural compound $BaNi_2P_2O_8$ [2].

The common expression for classical critical behavior near a phase transition at a temperature T_{c} is

$$\Delta H = C\left(\frac{T}{T_c} - 1\right)^{-p} + \Delta H_{\mathrm{lin}}. \quad (3)$$

Fitting the experimental data for $H \perp c$ with m fixed to the high-temperature value, and $T_c = T_{\mathrm{N}} = 50$ K held constant at the three-dimensional ordering temperature, we found a critical exponent $p = 2.3$, $C = 427$ Oe, and $\Delta H_0 = 610$ Oe. The same analysis for $H||c$, with fixed $p = 2.3$, yielded $C = 851$ Oe, and $\Delta H_0 = 1137$ Oe. Both of these fits are illustrated as dashed lines in Fig. 1. The linear plot of $\ln(\Delta H_{\mathrm{div}}) = \ln(\Delta H_{\mathrm{ESR}} - \Delta H_{\mathrm{lin}})$ vs $\ln(T/T_{\mathrm{N}} - 1)$ is shown in the middle frame of Fig. 2. The agreement of fit and data again is satisfactory.

Therefore, classical critical dynamics with a power-law behavior can describe the temperature dependence of the linewidth of $BaNi_2V_2O_8$ as well. The critical exponent is characteristic for the dimensionality of the fluctuations near the phase transition. Theoretical predictions for the critical exponent exist for the 3D Heisenberg ($p = 1.7$), the 3D Ising ($p = 1.8$), and the 2D Ising ($p = 3.3$) AFM [1], which all differ from our experimental value. However, the exponent observed in $BaNi_2V_2O_8$ is close to the empirical value found in several 2D magnets ($p = 2.6$), which are considered as good realizations of the 2D Heisenberg model with finite interplanar coupling [1]. It is interesting to note that an approximation of the theoretical expression for the linewidth at the KT transition by a critical behavior also yields $p \leq 3b/2 \approx 2.4$. This suggests that the observed critical increase of linewidth does not contradict the KT scenario. In a similar way the magnetization of the 2D XY model with finite interplanar coupling below T_{N} can be approximated by a critical behavior, which is compatible with the KT scenario and in agreement with experimental results in many real 2D systems [27].

For an isotropic $S = 1/2$ nearest-neighbor quantum Heisenberg AFM on a square lattice with a small interplanar coupling Chakravarty and Orbach [28] predicted

$$\Delta H_c(T) = F\left(\frac{\xi}{a}\right)^3 \frac{(k_B T/2\pi\rho_s)^{5/2}}{(1 + k_B T/2\pi\rho_s)^4} + \Delta H_{\text{lin}}, \quad (4)$$

where $\rho_s = kJ$ is the spin-stiffness constant with $k = 0.18$ for the spin-1/2 square lattice Heisenberg AFM [29], and ξ/a is the ratio of the temperature-dependent spin-correlation length to the spin-spin nearest-neighbor distance

$$\frac{\xi}{a} = \xi_0 \frac{\exp(2\pi\rho_s/k_B T)}{1 + k_B T/2\pi\rho_s}. \quad (5)$$

For $H \perp c$ with m fixed to the high-temperature value and $J/k_B = 96$ K this yields $k = 0.31$, $F = 2.5$, $\xi_0 = 3.5$, and $\Delta H_0 = 665$ Oe. The same analysis for $H||c$, with fixed $k = 0.31$ results in $F = 6.8$, $\xi_0 = 3.3$, and $\Delta H_0 = 2000$ Oe. The fitting curves are indicated as dotted lines in Fig. 1, and the lower frame of Fig. 2 shows both data and fits as a plot of $\ln(\Delta H_{\text{div}}) = \ln(\Delta H_{\text{ESR}} - \Delta H_{\text{lin}})$ vs T_N/T. In the region $1.25T_N$ to $2.5T_N$ the agreement is satisfactory. The results for $Cu(HCOO)_2 \cdot 4H_2O$, which were interpreted in terms of this model, suggest rather a pure $(\xi/a)^3$ dependence of ΔH than a behavior according to Eq. (4) [25]. Fitting our data with a pure $(\xi/a)^3$ term yields curves almost undistinguishable from those obtained by Eq. (4) with parameters $k = 0.25$, $\xi_0 = 2.5$ ($H \perp c$), and $\xi_0 = 3.3$ ($H \parallel c$), respectively. It is not surprising to find a qualitative agreement of the linewidth data with the prediction for the 2D Heisenberg model due to the only weak anisotropy of this compound. This is not in contradiction to the KT scenario, because our linewidth data are confined to the crossover regime between isotropic Heisenberg and disordered XY behavior.

Using ESR techniques we have investigated the temperature dependence of the linewidth in the 2D AFM $BaNi_2V_2O_8$. From previous magnetic and thermodynamic measurements [20] we supposed that $BaNi_2V_2O_8$ is a 2D Heisenberg AFM with weak easy-plane exchange anisotropy [12,13]. The ESR measurements confirm the 2D properties of the spin dynamics: The divergent behavior of $\Delta H(T)$ on approaching the 3D AFM phase transition from above can be well described in terms of the 2D Heisenberg AFM. However, such a system still undergoes a KT transition with a preceding temperature range of disordered XY behavior [10]. This region is increased by an applied magnetic field [14] as used in ESR measurements. Because of this the data can be described very well in the KT scenario revealing the predicted value $b = \pi/2$. We arrive at a KT temperature $T_{KT} = 43.3$ K ($t_{KT} = 0.2$), well below the 3D ordering temperature. Based on these arguments, we conclude that the experimental results are fully compatible with the presence of a KT transition in $BaNi_2V_2O_8$.

This work was supported by the German Bundesministerium für Bildung und Forschung (BMBF) under Contract No. VDI/EKM 13N6917 and by the Deutsche Forschungsgemeinschaft (DFG) via the Sonderforschungsbereich (SFB) 484. We gratefully acknowledge useful discussions with H. Benner (TU Darmstadt, Germany) and D. Huse (Princeton University, NJ). The work at Princeton was supported by the National Science Foundation, Grant No. DMR-9809483.

[1] H. Benner and J. P. Boucher, in *Magnetic Properties of Layered Transition Metal Compounds*, edited by L. J. de Jongh (Kluwer Academic Publishers, Dordrecht/Boston/London, 1990), pp. 323–378.
[2] L. P. Regnault and J. Rossat-Mignod, in *Magnetic Properties of Layered Transition Metal Compounds* (Ref. [1]), pp. 271–321.
[3] N. D. Mermin and H. Wagner, Phys. Rev. Lett. **17**, 1133 (1966).
[4] J. M. Kosterlitz and D. J. Thouless, J. Phys. C **6**, 1181 (1973).
[5] J. M. Kosterlitz, J. Phys. C **7**, 1046 (1974).
[6] V. L. Berezinskii, Sov. Phys. JETP **32**, 493 (1971).
[7] V. L. Berezinskii, Sov. Phys. JETP **34**, 610 (1972).
[8] L. H. de Jongh, in *Magnetic Properties of Layered Transition Metal Compounds* (Ref. [1]), pp. 1–51.
[9] S. Hikami and T. Tsuneto, Prog. Theor. Phys. **63**, 387 (1980).
[10] T. Roscilde *et al.*, Phys. Status Solidi B **236**, 433 (2003).
[11] A. Cuccoli *et al.*, Phys. Rev. B **52**, 10 221 (1995).
[12] A. Cuccoli *et al.*, Phys. Rev. Lett. **90**, 167205 (2003).
[13] A. Cuccoli *et al.*, Phys. Rev. B **67**, 104414 (2003).
[14] A. Cuccoli *et al.*, cond-mat/0302440.
[15] K. Okuda *et al.*, J. Phys. Soc. Jpn. **55**, 4456 (1986).
[16] H. M. Rønnow *et al.*, Physica (Amsterdam) **276B–278B**, 676 (2000).
[17] J. Becker, Ph.D. thesis, TU Darmstadt, Germany, 1996.
[18] P. Gaveau *et al.*, J. Appl. Phys. **69**, 6228 (1991).
[19] L. P. Regnault *et al.*, J. Magn. Magn. Mater. **31–34**, 1205 (1983).
[20] N. Rogado *et al.*, Phys. Rev. B **65**, 144443 (2002).
[21] A. Cuccoli *et al.*, Phys. Rev. B **56**, 14 456 (1997).
[22] L. Capriotti *et al.*, J. Appl. Phys. **81**, 4137 (1997).
[23] H.-A. Krug von Nidda *et al.*, Phys. Rev. B **65**, 134445 (2002).
[24] T. G. Castner, Jr. and M. S. Seehra, Phys. Rev. B **4**, 38 (1971).
[25] T. G. Castner and M. S. Seehra, Phys. Rev. B **47**, 578 (1993).
[26] F. G. Mertens *et al.*, Phys. Rev. B **39**, 591 (1989).
[27] S. T. Bramwell and P. C. W. Holdsworth, J. Phys. Condens. Matter **5**, L53 (1993).
[28] S. Chakravarty and R. Orbach, Phys. Rev. Lett. **64**, 224 (1990).
[29] R. R. P. Singh and D. A. Huse, Phys. Rev. B **40**, 7247 (1989).